

CFD Assessment of Combined Heat and Power Plants with Various Outlet Collection Altitudes

Ujjawal Ranjan¹, Prof. Amit Kumar Singh²

¹Ujjawal Ranjan, Department of ME, Truba Institute of Engineering and Information Technology, Bhopal (M.P), India

²Prof. Amit Kumar Singh, Department of ME, Truba Institute of Engineering and Information Technology, Bhopal (M.P), India

ujjawalranjan108@gmail.com, amit821991@gmail.com

* Corresponding Author: Ujjawal Ranjan

Abstract: In this study, computational fluid dynamics analyses of combined heat and power plants with various outlet collector heights ($H_2 = 1.85\text{ m}$, 3 m , 4 m , and 5 m) and radially curving on collectors roofs of 10 m and 20 m were carried out. The outlet collector height is changed to change both roofing slope and curving diameter of the collection, while the input hoarder height is set at $H_1 = 1.85\text{ m}$ of solar chimney power plant at varied radiation from the sun including such 1000 W/m^2 , 800 W/m^2 , 600 W/m^2 , 400 W/m^2 , and 200 W/m^2 . For this, a three-dimensional axially symmetric CAD model was created.

Keywords: solar chimney, collector, radial height, radiations, CAD

I. Introduction

A solar chimney power station is an electricity device that generates electricity by using the buoyant of something like the air. A chimneys, a collection bowl, as well as a generator are the three primary components of photovoltaic towers. The collection is composed of a clear material like polypropylene or acrylic and is placed a few metres above ground. The collectors covers a broad region, and its diameter with one kilometer is not rare. The chimneys is situated in the center of the point of collection, many hundred yards away. The generator is positioned in which the chimneys joins the collectors just at bottom of something like the chimney construction. Solar radiation enters the substance throughout the day and warms the air in between sensors and indeed the floor. Heat alters the volume of the air, causing it to move and expand, resulting in a pressure differential in the system. The convective heat circulate in the collectors and exhaust, while air temperature from outside is taken into the manifold. The upward flow of the air from the collection to the exhaust is sufficient to power a turbine. Using subterranean energy storage, the quantity of heat emitted from the subsurface can be enhanced [3]. Heat storage technologies capture energy from the sun and use it to accelerate heat transport in the air. The majority of storage technologies are constructed of materials that have a superior temperature capacity. As sealed freshwater canisters that are either stored below surface or submerged below subterranean. Solar wind turbines are an efficient way to generate power from solar energy [5]. They also require very little upkeep. The concentrated solar power sensor does not need to be cleaned because it is utilized to control the temperature, which decreases running expenses when contrasted to solar panels, which do. A distinctive aspect of solar present system is that the space here between sensors as well as the substrate can act as a greenhouses [5]. Only 1% to 2% of the power generation system is converted into mechanical energy that may be utilised by the rotor for solar energy [3]. Power stations with a large solar collectors and a tall chimney are necessary to extract more electricity from the chimneys network.

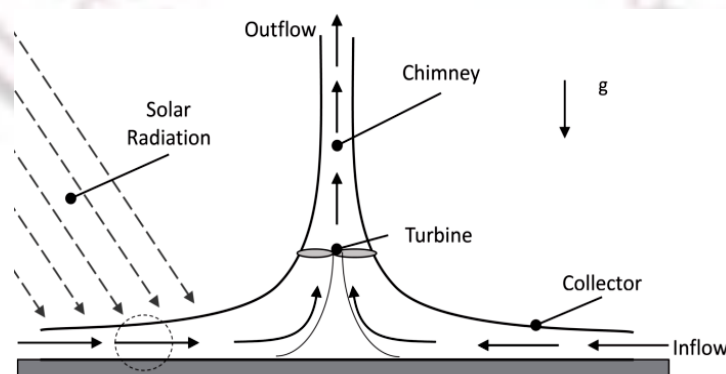


Figure 1 Schematic diagram of solar chimney power plant

II. Literature Review

Ammar Mebarki et al. (2022) [1] The goal of this article is to provide a database for proper SCPP integration in metropolitan areas. A 3D axisymmetric CFD model for the SCPP at Manzanares, Spain, was provided to prove that the

assessment. Six chimney models were decreased by a factor of 0.5 and exposed to various levels of solar radiation, yielding 30 possibilities. The RNG k-turbulence model was used, as well as the discontinuous coordinates non-grey irradiation simulation. The study also includes an illustration of how the findings were used to evaluate daily power production from planned chimneys upon that roofs of shop houses. As the scale factor decreases, production power and systems effectiveness follow a power and exponential drop, correspondingly. For scale factors of 0.76, 0.636, and 0.51, correspondingly, exposure to ionizing radiation of 1000 w/m² generates 21.2, 11.74, and 5.65 kW/h electrical power. In Batna, Algeria, they supply daily energy of 191.93, 106.55, and 51.12 kWh/day on a day type.

Omer K. Ahmed et al. (2022) [2] Solar chimney systems integrated with other renewables or traditional energy sources are the subject of the contemporary review study. This article focused on compressed solar smokestacks with photovoltaic arrays, solar water features, and geothermal heat, as well as a demonstration of hybrid renewable energy systems that were incorporated with power plants. The efficiency of these photovoltaic energy chimney is quantified, potential obstacles are identified, and academics are given insights into designs that have been presented in recent times. Recommendations for optimizing the productivity of solar hybrid chimney have already been made.

Tianhe Long et al. (2022) [3] The solar condenser, basic natural convective regenerator (NCR), and convection configuration with a horizontal sun chimneys are the three main types of regenerators (NCR-SC). The boost in weight conversion efficiency due to the solar chimney's variable viscosity is plainly visible. When opposed to the thermal convection steam generator, the data demonstrate that miserable weather has a far more substantial detrimental influence on the solar still. Due to variable viscosity, the convection mass flow rate of the NCR-SC rose by 32% on August 20th compared to the NCR. In the case of high atmospheric wind speeds (only 16% on August 25th), this increase would've been decreased. The concentrated solar inefficiencies of the NCR-SC are the highest (57.8% e64.6%), following by that of the NCR (48.4% e58.9%), while the concentrated solar inefficiencies are still the lowest (30.3% e38.5%).

Bouchair (2022) [4] Simulation and hardware analysis and quantitative computation, the goal of this study was to demonstrate the correlation among height and solar chimneys effectiveness. Mathematical modeling of heat conduction transport from adiabatic vertical sides of a chimney. To address the problem of the equation's non-linearity, a Matlab application was created. If we assume a consistent temperature of air for all elevations, the results demonstrate that height has a minor but significant impact on the effectiveness of the solar chimney. However, in real-world weather conditions, the ambient temperature is affected by height. The altitude has a major impact on the functioning of the heat exchanger in these conditions. Microclimatic variables, but instead of large-scale region meteorological factors, should be employed to build solar chimneys.

Seyyed Hossein Fallah & Mohammad Sadegh Valipour (2022) [5] Experimental values from the library were used to confirm the simulations. For natural sunlight exceeding 600 W/m² from morning to midday, simulation results demonstrate that quasi - steady circulation was an appropriate hypothesis. Furthermore, for solar radiation of 800 W/m², the highest air movement in a sloping solar chimney power plant where its chimney's entry is 2.73 m/s was reported. Finally, investigations showed that by reducing the elevation of the chimneys by 25% (from 9 to 2.25 m), the maximal airspeed was massively reduced from 2.73 to 2.07 m/s, while the average annual temperature there at fireplace entry increased modestly by approximately 1%.

Cristiana Brasil Maia & Janaina de Oliveira Castro Silva (2022) [6] The mass flow rate of water and temperature levels of the airflow are predicted using a theoretical formulation on an hourly basis over the course of a year, and the results demonstrate excellent agreement data acquired in a tiny prototype. The system's performance was tested, with an enhanced energy effectiveness of 11%. The prototype's modest proportions were blamed for the prototype's low exergoeconomic efficiency.

A.T. Layeni et al. (2021) [7] In this work, sensitivity analysis was performed using the ANSYS Fluent CFD package in conjunction with the statistical program "Design Expert" to determine the possibilities of the SC system for structures. On a 4 m 4 m 4 m room, a 23 random experimentation was modeled and analyzed. The influence of interconnections of parameter parameters of the SC, chimneys elevation, width, and Solar thermal flux, was found to be quite important in the modeled experimental analysis. The SC produces roughly 25 W/m² of power and has a stream velocity of 1.5 m/s. The room temperature is maintained at 300 K, but the gravitational acceleration in the room was increased to around 1.5 m/s.

A Vazquez-Ruiz et al. (2021) [8] A numerical-experimental investigation of heat transfer and airflow in a scaling space with a heater surface or a double horizontal rooftop solar chimneys is presented in this paper. A parametric research was conducted in the thermal performance for the laboratory experiment, taking into account varying amounts of heat flux delivered to a vertical surface of the sized chamber and six distinct placements of the rooftop photovoltaic chimneys. For both heat source, empirical temperature distribution were collected at six various depths and elevations, and empirical heat transfer rate were calculated. Using computer simulation software, the mathematical formalism group k-epsilon flow and heat transfer was compared to experimental evidence.

Carlos Mendez & Yusuf Bicer (2021) [9] The viability of developing an integrated system for energy and freshwater generation, with hybrid renewable energy technologies as its major pillar, is examined in this study. To examine electricity production and heat transmission to the solar chimney's storage solution, a rough estimate literature and studies is conducted. A saltwater desalination process system is also included, with the goal of increasing the photovoltaic chimney's total efficiency. A geothermal power systems with a hydraulic turbine is also included to provide electricity and groundwater requirements without interruptions. As a result, installing an integrated solution with a solar

chimney as its primary energy source yields an energy conversion efficiency of 8.4%, which is significantly greater than an individual solar chimney.

D.M. Aliaga et al. ((2021) [10]A improved solar chimney's effectiveness is investigated mathematically and experimentally. The traditional collector arrays is supplemented in this solar air heater with a heating element placed in the center part. The professional Computational Fluid Dynamics (CFD) code COMSOL simulates convective heat transfer inside. This application is first used to conduct a peak power optimisation and select the best proportions for the chimneys prototypes. A two-meter high pyramid model is created using the computationally determined parameters to monitor temperature distribution and energy density of the column. The disparity among theoretically and experimentally data for the electricity produced is less than 6.2 percent..In contrast to earlier published prototype built on a typical solar chimneys design of normal stature, our model obtains a better conversion efficiency.

According to the above literary works, a lot of research has been performed by investigators utilizing unconventional, case study, mathematical, and numerical simulations to enhance the productivity of the SCPP, and research is still ongoing to enhance the productivity of the SCPP, so there is a lot of room for more work in the industry

III.METHODOLOGY

The solar chimney power station is a sustainable electrical power station that involves reducing solar warmth to generate electricity. To generate energy, this circulation powers wind generators situated within in the column updraft or surrounding the column base. For computer simulation investigation, multiple models of solar chimneys with collectors draft and staircase draft have really been constructed.

The current research is divided into two sections: mathematics research and simulation software analysis. The following parameters were estimated using a theoretical version that was upgraded to progressed: power output, maximum chimney height, circulation temperatures, speed, and system effectiveness. ANSYS software was used to model the solar thermal power plant in CAD.Because the goal is to enhance energy output, the width of something like the absorber plate is also regarded an optimal value. Parametric experiments were also carried out to see how the distance between the collector and the ground affected the generating capacity. For the both systems, an optimal separation is established.

CAD Modeling of Solar chimney power plant

SCPP with collector height $H_1 = H_2 = 1.85$ mat radial curvature of collector roof is 10 m:

With the help of Solidworks software, a quarter of a three-dimensional Model data of a solar water heating system was constructed in this project. As indicated in figure 2, the chimneys height is 194.6 meters, the chimney radius is 8.05 meters, the collection diameter is 122 meters, and the collectors elevation is $H_1 = H_2 = 1.85$ meters. The circumferential curve of the collectors roof is 10 meters.

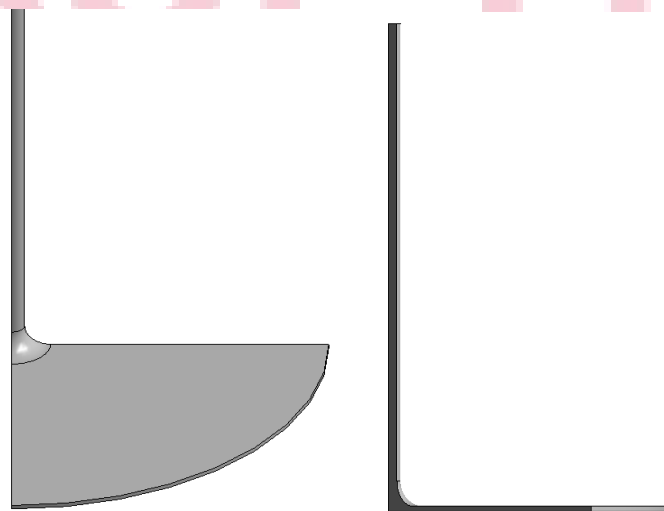


Figure 2 CAD model of Solar chimney power plant with collector height $H_1 = H_2 = 1.85$ mat radial curvature of collector roof is 10 m

SCPP with collector height $H_1 = 1.85$ m & $H_2 = 3$ mat radial curvature of collector roof is 10 m:

With both the help of Solidworks software, a quarter of a three-dimensional Cad system of a hybrid energy storage system was constructed in this project. The dimensions are considered: chimneys height 194.6 m, chimney radius 8.05 m, collectors diameter 122 m, collector height $H_1 = 1.85$ m & $H_2 = 3$, and radial curving of collectors roof 10 m, as illustrated in figure 3.

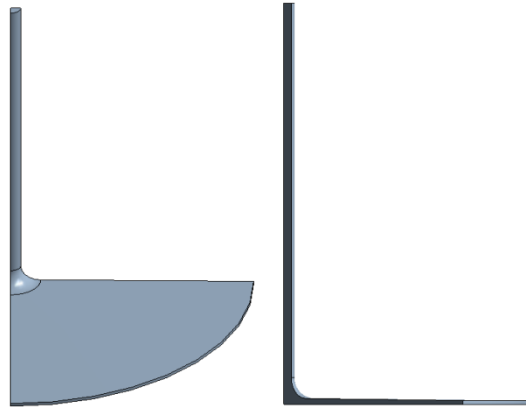


Figure 3 CAD model of SCPP with collector height $H_1 = 1.85$ m & $H_2 = 3$ mat radial curvature of collector roof is 10 m

SCPP with collector height $H_1 = 1.85$ m & $H_2 = 4$ mat radial curvature of collector roof is 10 m:

With the help of Solid works software, a quarter of a three-dimensional Cad system of a solar water heating system was constructed in this project. The components are as follows: chimneys height 194.6 m, chimneys diameter 8.05 m, collectors diameter 122 m, collector height $H_1 = 1.85$ m & $H_2 = 4$, and radial curve of collectors roof 10 m, as illustrated in figure 4.

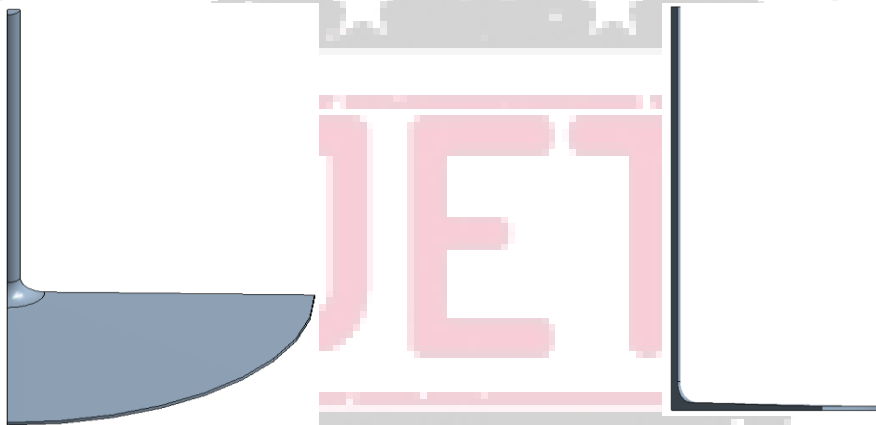


Figure 4 : CAD model of SCPP with collector height $H_1 = 1.85$ m & $H_2 = 4$ mat radial curvature of collector roof is 10 m

SCPP with collector height $H_1 = 1.85$ m & $H_2 = 5$ mat radial curvature of collector roof is 10 m:

With the help of Ansys software, a quarter of a three-dimensional CAD model of a solar water heating system was constructed in this project. The dimensions are considered: chimneys height 194.6 m, chimneys diameter 8.05 m, collectors circle 122 m, collector height $H_1 = 1.85$ m & $H_2 = 5$, and radial curve of collectors roof 10 m, as illustrated in figure 5.

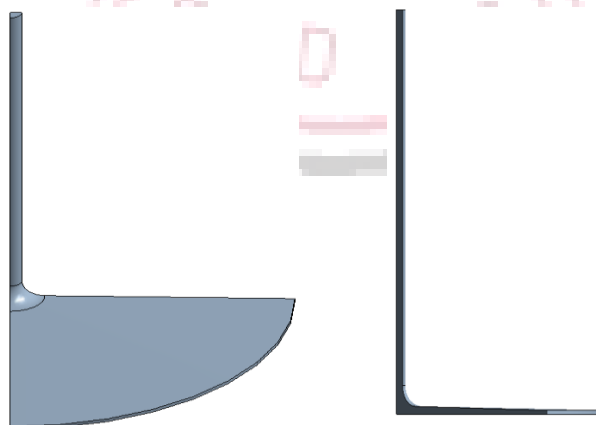


Figure 5: CAD model of SCPP with collector height $H_1 = 1.85$ m & $H_2 = 5$ m at radial curvature of collector roof is 10 m

SCPP with collector height $H_1 = H_2 = 1.85$ m at radial curvature of collector roof is 20 m:

With the help of Solid works software, a quarter of a three-dimensional CAD system of a solar water heating system was constructed in this project. As indicated in figure 6, the chimneys height is 194.6 meters, the fireplace radius is 8.05 meters, the collection diameter is 122 meters, the collector height is $H_1 = H_2 = 1.85$ metres high, as well as the circumferential curve of the collectors roof is 20 meters.

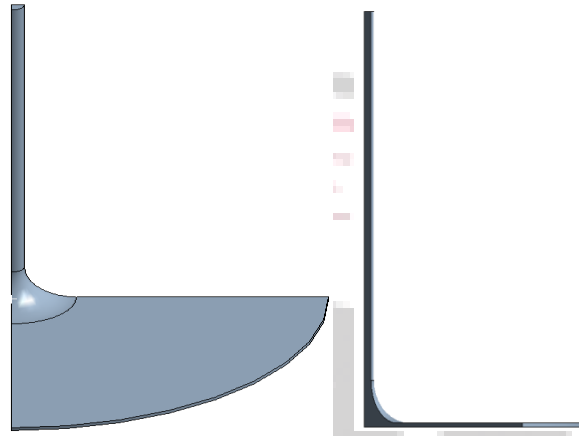


Figure 6: CAD model of SCPP with collector height $H_1 = H_2 = 1.85$ m at radial curvature of collector roof is 20 m

SCPP with collector height $H_1 = 1.85$ m & $H_2 = 3$ m at radial curvature of collector roof is 20 m: With the help of Ansys software, a quarter of a three-dimensional CAD model of a solar water heating system was constructed in this project. The following are the volumetric specifications: chimneys height 194.6 m, chimney radius 8.05 m, collectors diameter 122 m, collectors elevation $H_1 = 1.85$ m & $H_2 = 3$ m, and circumferential curve of collectors roof 20 m, as can be seen in figure no. 7.

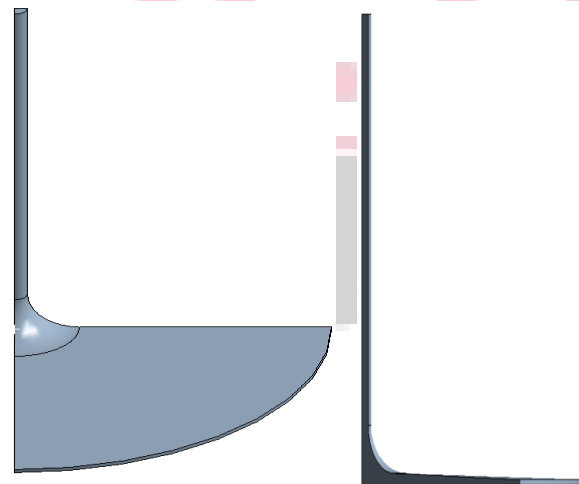


Figure 7: CAD model of SCPP with collector height $H_1 = 1.85$ m & $H_2 = 5$ m at radial curvature of collector roof is 20 m

IV. RESULT AND DISCUSSION

In this study, computer simulation analyses of concentrated solar power plants with various outlet collection heights ($H_2 = 1.85$ m, 3 m, 4 m, and 5 m) and radially curving on collectors roofs of 10 m and 20 m were carried out. At various solar irradiance such as 1000 W/m², 800 W/m², 600 W/m², 400 W/m², and 200 W/m², the roof slope and curving diameter of the collectors can be changed by altering the output collection height, while the input collectors height is fixed as $H_1 = 1.85$ m of solar water heating system.

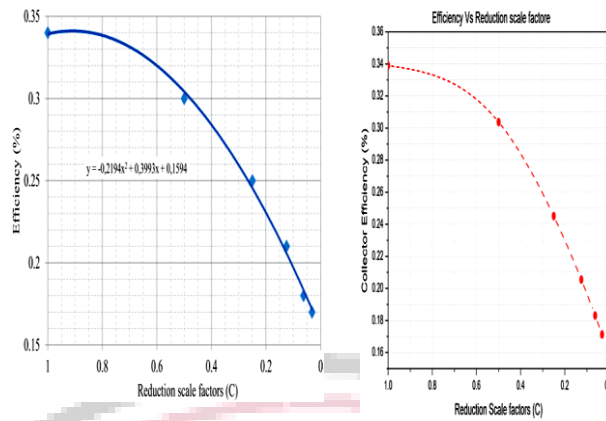


Figure: 8 (a): Collector Efficiency [Ammar et al 2022]

Figure: 8 (b): Collector Efficiency [Present work]

After performing CFD analysis the collector efficiency of the solar chimney power plant at different reduction factor have been observed and compared with the base paper as shown in figure 8 (a) & (b) with maximum variation of 5.05% which show very good agreement with base paper and present work.

Results for CFD analysis of solar chimney power plant at collector height 1.85 m and radial curvature of collector roof is 10 m:

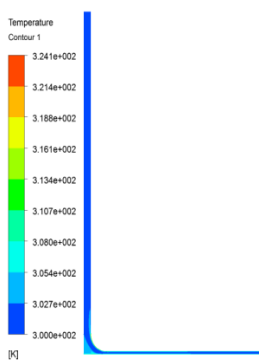


Figure 9 : Temperature distribution on SCPP for with collector height $H_2 = 1.85 \text{ m}$ & $R = 10 \text{ m}$ at 1000 W/m^2

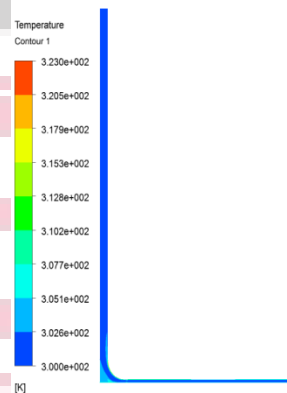


Figure 10: Temperature distribution on SCPP for with collector height $H_2 = 1.85 \text{ m}$ & $R = 10 \text{ m}$ at 800 W/m^2

Combined heat and power station simulation software simulation for base model with collector height $H_2 = 1.85 \text{ m}$ and solar radioactive waste of 1000 W/m^2 and 800 W/m^2 . Figures 9 and 10 showed that maximum temperatures within the heat exchanger was 324.1 K for 1000 W/m^2 and 323.0 K for 800 W/m^2 .

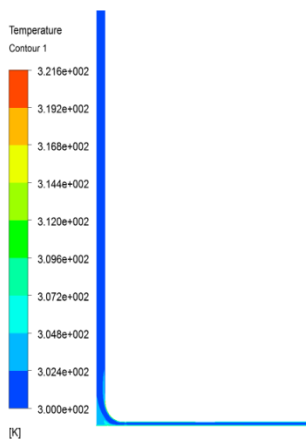


Figure 11: Temperature distribution on SCPP for with collector height $H_2 = 1.85 \text{ m}$ & $R = 10 \text{ m}$ at 600 W/m^2

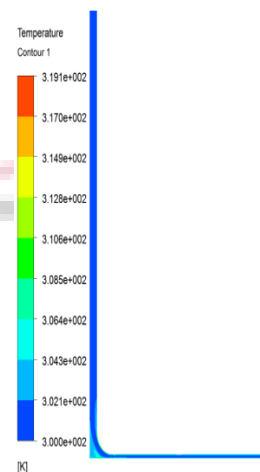


Figure 12: Temperature distribution on SCPP for with collector height $H_2 = 1.85 \text{ m}$ & $R = 10 \text{ m}$ at 400 W/m^2

Concentrated solar power plant simulation software simulation for base model with collector height $H_2 = 1.85$ m and solar radiations of 600 W/m^2 and 400 W/m^2 . As illustrated in figures 11 and 12, the solar chimney reached maximum temperatures of 321.6 K and 319.1 K . Concentrated solar power plant simulation software simulation using base model with collectors height $H_2 = 1.85$ m and solar radiations of 200 W/m^2 . Figure 13 represents the highest temperatures observed on the inside of the solar chimney, which was 318.2 K .

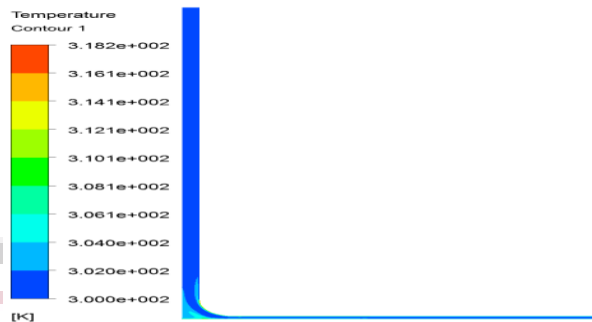


Figure 13: Temperature distribution on SCPP for with collector height $H_2 = 1.85$ m & $R = 10$ m at 200 W/m^2

Results for CFD analysis of solar chimney power plant at collector height 3 m and radial curvature of collector roof is 10 m:

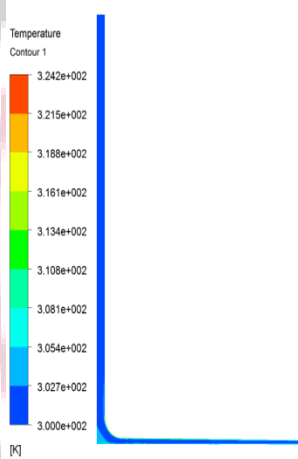


Figure 14: Temperature distribution on SCPP for with collector height $H_2 = 3$ m & $R = 10$ m at 1000 W/m^2

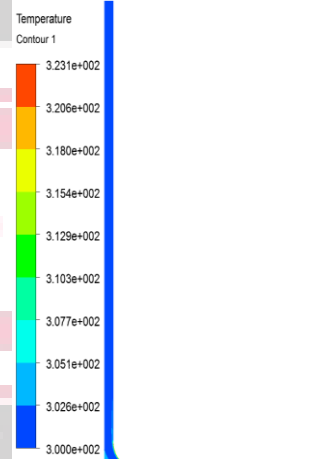


Figure 15: Temperature distribution on SCPP for with collector height $H_2 = 3$ m & $R = 10$ m at 800 W/m^2

Concentrated solar power plant simulation software simulation for base model at collector height $H_2 = 3$ m and solar radiations of 1000 W/m^2 and 800 W/m^2 . Figures 14 and 15 indicated that the maximum temperatures within the heat exchanger was 324.2 K for 1000 W/m^2 and 323.1 K for 800 W/m^2 .

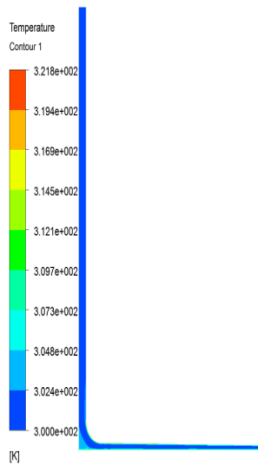


Figure 16: Temperature distribution on SCPP for with collector height $H_2 = 3$ m & $R = 10$ m at 600 W/m^2

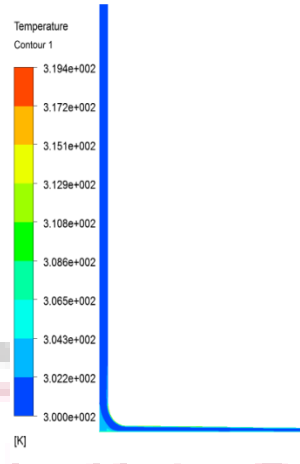


Figure 17: Temperature distribution on SCPP for with collector height $H_2 = 3$ m & $R = 10$ m at 400 W/m^2

Concentrated solar power plant simulation software simulation for base model with collector height $H_2 = 3$ m and solar radionuclides of 600 W/m^2 and 400 W/m^2 . Figures 16 and 17 indicate the maximum temperatures of 321.8 K and 319.4 K , respectively, inside the photovoltaic panel. Combined heat and power station simulation software analysis for base model with collectors height $H_2 = 3$ m and solar radionuclides of 200 W/m^2 . Figure 18 represents the highest temperatures of 318.4 K observed inside the photovoltaic panel.

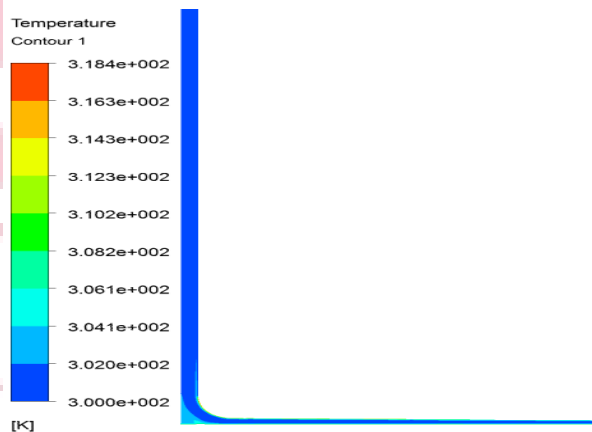


Figure 18: Temperature distribution on SCPP for with collector height $H_2 = 3$ m & $R = 10$ m at 200 W/m^2

Results for CFD analysis of solar chimney power plant at collector height 4 m and radial curvature of collector roof is 10 m:

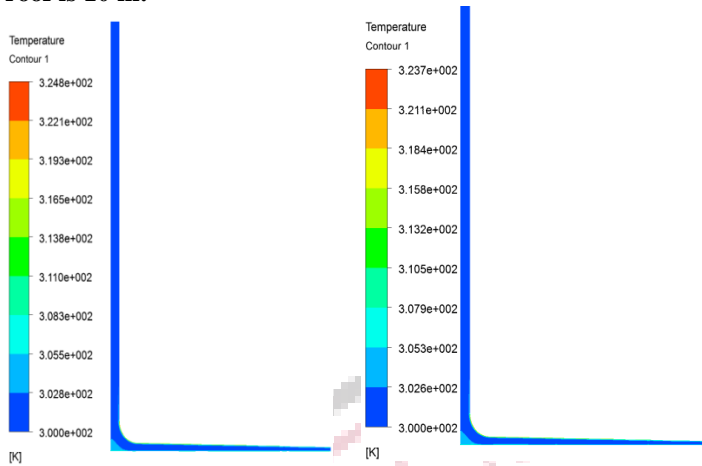


Figure 19: Temperature distribution on SCPP for with collector height $H_2 = 4$ m & $R = 10$ m at 1000 W/m^2

Figure 20: Temperature distribution on SCPP for with collector height $H_2 = 4$ m & $R = 10$ m at 800 W/m^2

Combined heat and power station simulation software simulation for base model at collector height $H_2 = 4$ m and solar radionuclides of 1000 W/m^2 and 800 W/m^2 . Figures 19 and 20 showed that maximum temperatures within the solar chimney was 324.8 K for 1000 W/m^2 and 323.7 K for 800 W/m^2 .

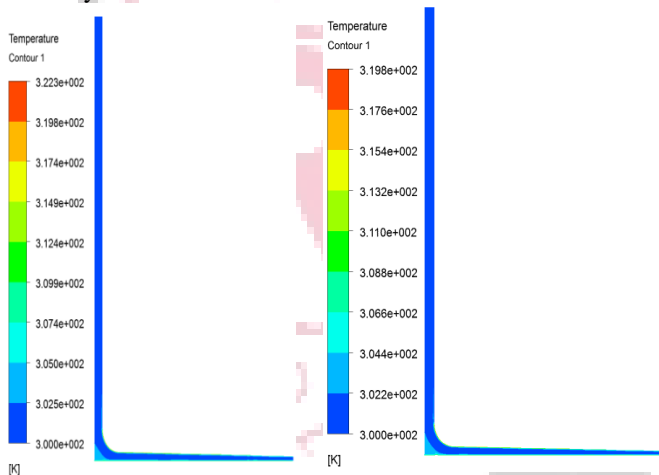


Figure 21: Temperature distribution on SCPP for with collector height $H_2 = 4$ m & $R = 10$ m at 600 W/m^2

Figure 22: Temperature distribution on SCPP for with collector height $H_2 = 4$ m & $R = 10$ m at 400 W/m^2

Concentrated solar power plant simulation software evaluation for baseline model with collector height $H_2 = 4$ m and solar radionuclides of 600 W/m^2 and 400 W/m^2 . Figures 21 and 22 represent the maximum temperatures of 322.3 K and 319.8 K , respectively, on the inside of the photovoltaic panel. Concentrated solar power plant simulation software evaluation for base model with collector height $H_2 = 4$ m and solar radiations of 200 W/m^2 . Figure 23 represents the highest temperatures observed on the inside of the solar chimney, which was 318.9 K .

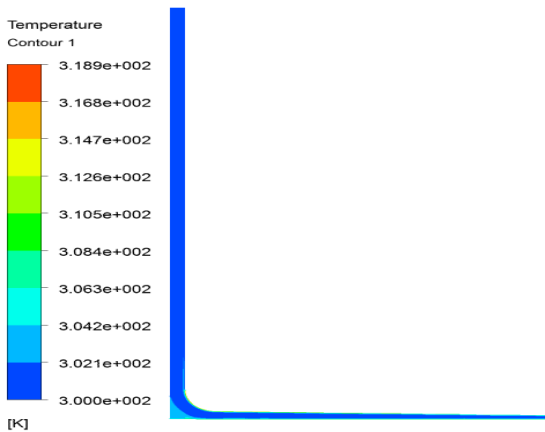


Figure 23: Temperature distribution on SCPP for with collector height $H_2 = 4\text{ m}$ & $R = 10\text{ m}$ at 200 W/m^2 Results for CFD analysis of solar chimney power plant at collector height 5 m and radial curvature of collector roof is 10 m:

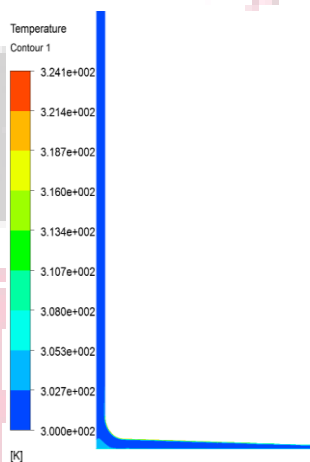
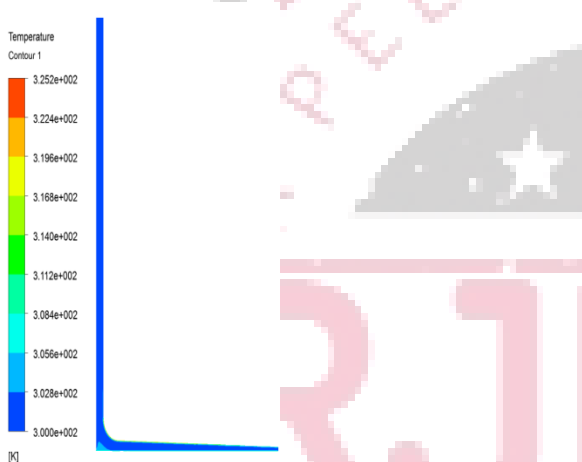


Figure 24: Temperature distribution on SCPP for with collector height $H_2 = 5\text{ m}$ & $R = 10\text{ m}$ at 1000 W/m^2

Figure 25: Temperature distribution on SCPP for with collector height $H_2 = 5\text{ m}$ & $R = 10\text{ m}$ at 800 W/m^2

Combined heat and power station simulation software simulation for base model at collector height $H_2 = 5\text{ m}$ and solar radionuclides of 1000 W/m^2 and 800 W/m^2 . Figures 24 and 25 show that the average temperature within the photovoltaic panel was 325.2 K for 1000 W/m^2 and 324.1 K for 800 W/m^2 .

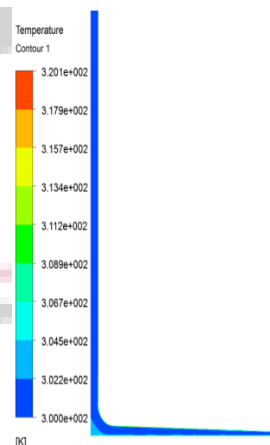
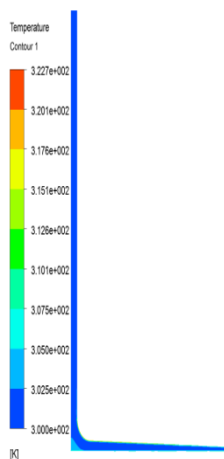


Figure 26: Temperature distribution on SCPP for with collector height $H_2 = 5\text{ m}$ & $R = 10\text{ m}$ at 600 W/m^2

Figure 27: Temperature distribution on SCPP for with collector height $H_2 = 5\text{ m}$ & $R = 10\text{ m}$ at 400 W/m^2

Concentrated solar power plant simulation software simulation for base model with collector height $H_2 = 5\text{ m}$ and solar radiations of 600 W/m^2 and 400 W/m^2 . Figures 26 and 27 indicate the maximum temperatures of 322.7 K and 320.1 K ,

respectively, inside the solar chimney. Concentrated solar power plant simulation software analysis using base model at collectors height $H_2 = 5$ m and solar radionuclides of 200 W/m^2 . Figure 28 represents the highest temperatures observed on the inside of the heat exchanger, which was 319.1 K .

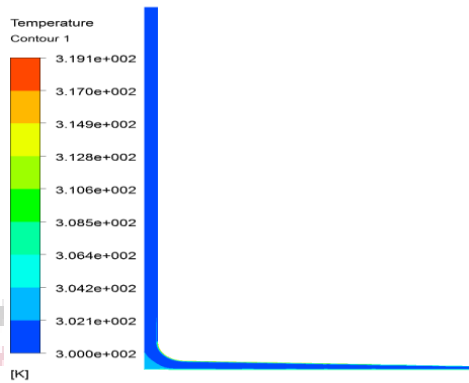


Figure 28: Temperature distribution on SCPP for with collector height $H_2 = 5$ m & $R = 10$ m at 200 W/m^2
Results for CFD analysis of solar chimney power plant at collector height 1.85 m and radial curvature of collector roof is 20 m:

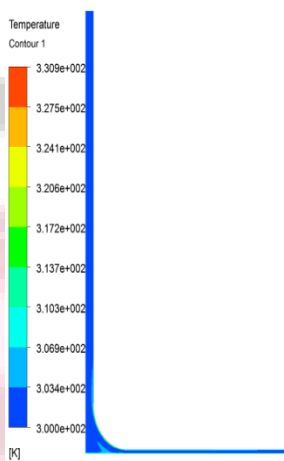


Figure 29 : Temperature distribution on SCPP for with collector height $H_2 = 1.85$ m & $R = 20$ m at 1000 W/m^2

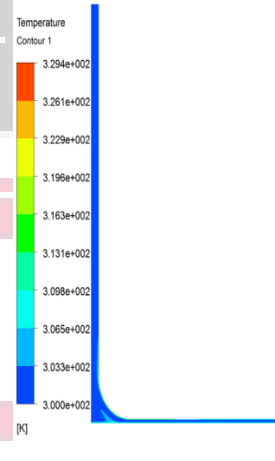


Figure 30: Temperature distribution on SCPP for with collector height $H_2 = 1.85$ m & $R = 20$ m at 800 W/m^2

Solar thermal power station simulation software simulation for baseline model with collectors height $H_2 = 1.85$ m and solar radioactive waste of 1000 W/m^2 and 800 W/m^2 . Figures 29 and 30 showed that maximum temperatures within the photovoltaic panel was 330.9 K for 1000 W/m^2 and 329.4 K for 800 W/m^2 .

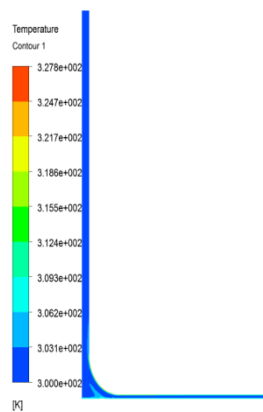


Figure 31: Temperature distribution on SCPP for with collector height $H_2 = 1.85$ m & $R = 20$ m at 600 W/m^2

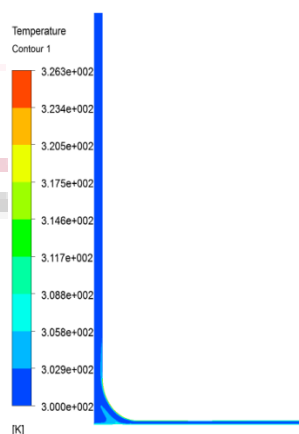


Figure 32: Temperature distribution on SCPP for with collector height $H_2 = 1.85$ m & $R = 20$ m at 400 W/m^2

Solar chimney power plant simulation software simulation for base model with collector height $H_2 = 1.85$ m and solar radioactive waste of 600 W/m^2 and 400 W/m^2 . Figures 31 and 32 represent the maximum temperatures of 327.8 K and 326.3 K , respectively, inside the photovoltaic panel.

Solar thermal power plant simulation software simulation for base model with collector height $H_2 = 1.85$ m and solar radiations of 200 W/m^2 . Figure 33 represents the highest temperatures observed inside the photovoltaic panel, which was 324.8 K .

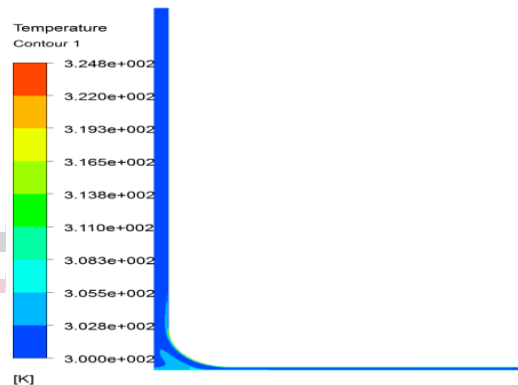


Figure 33: Temperature distribution on SCPP for with collector height $H_2 = 1.85$ m & $R = 20$ m at 200 W/m^2

Results for CFD analysis of solar chimney power plant at collector height 3 m and radial curvature of collector roof is 20 m:

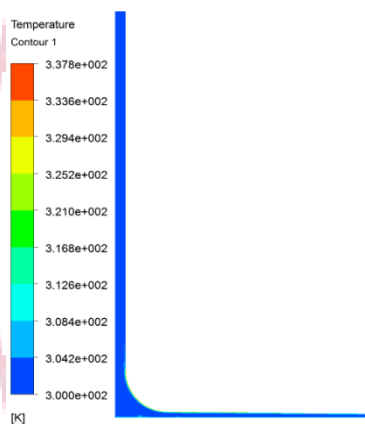


Figure 34 : Temperature distribution on SCPP for with collector height $H_2 = 3$ m & $R = 20$ m at 1000 W/m^2

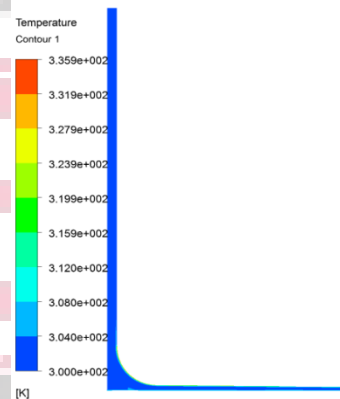


Figure 35: Temperature distribution on SCPP for with collector height $H_2 = 3$ m & $R = 20$ m at 800 W/m^2

Solar chimney power plant simulation software simulation for base model at collectors height $H_2 = 3$ m and solar gamma radiation of 1000 W/m^2 and 800 W/m^2 . Figures 34 and 35 show that the hottest temperature within the solar chimney was 337.8 K for 1000 W/m^2 and 335.9 K for 800 W/m^2 .

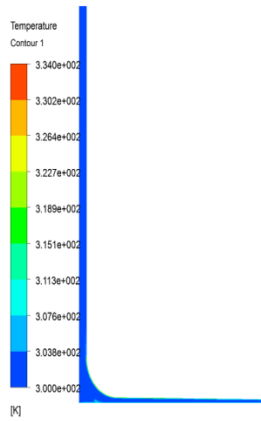


Figure 36: Temperature distribution on SCPP for with collector height $H_2 = 3\text{ m}$ & $R = 20\text{ m}$ at 600 W/m^2

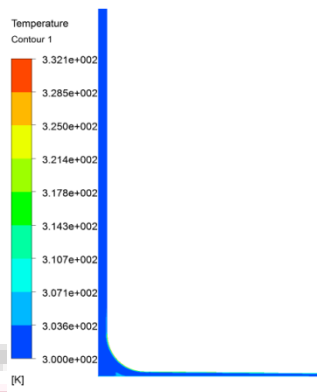


Figure 37: Temperature distribution on SCPP for with collector height $H_2 = 3\text{ m}$ & $R = 20\text{ m}$ at 400 W/m^2

Solar chimney power station simulation software simulation for base model with collectors height $H_2 = 3\text{ m}$ and solar radionuclides of 600 W/m^2 and 400 W/m^2 . Figures 36 and 37 represent the maximum temperatures of 334.0 K and 332.1 K , respectively, inside the photovoltaic panel.

Combined heat and power plant simulation software simulation for baseline model with collector height $H_2 = 3\text{ m}$ and solar radiations of 200 W/m^2 . Figure 38 shows a maximum temperatures observed inside the solar chimney, which was 330.2 K .

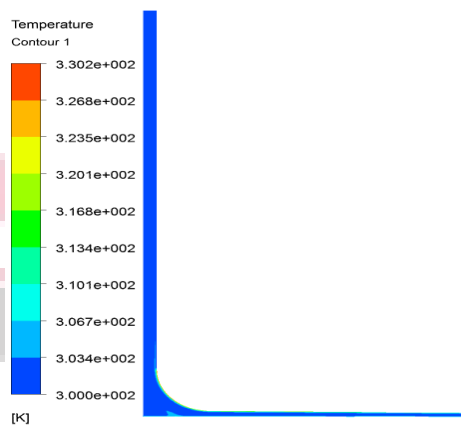


Figure 38 : Temperature distribution on SCPP for with collector height $H_2 = 3\text{ m}$ & $R = 20\text{ m}$ at 200 W/m^2

Results for CFD analysis of solar chimney power plant at collector height 4 m and radial curvature of collector roof is 20 m:

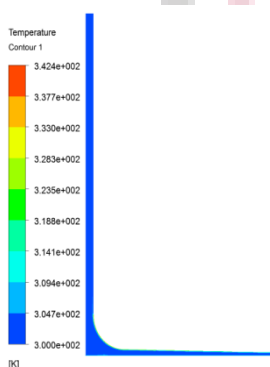


Figure 39: Temperature distribution on SCPP for with collector height $H_2 = 4\text{ m}$ & $R = 20\text{ m}$ at 1000 W/m^2

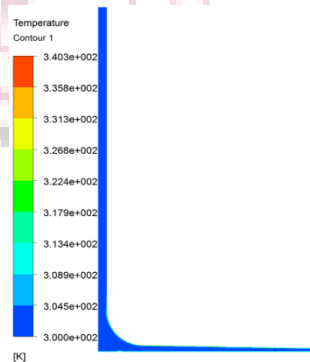


Figure 40: Temperature distribution on SCPP for with collector height $H_2 = 4\text{ m}$ & $R = 20\text{ m}$ at 800 W/m^2

Solar chimney power plant simulation software simulation for baseline model at collectors height $H_2 = 4$ m and solar radioactive isotopes of 1000 W/m^2 and 800 W/m^2 . Figures 39 and 40 show that the highest temperatures within the photovoltaic panel was 342.4 K for 1000 W/m^2 and 340.3 K for 800 W/m^2 .

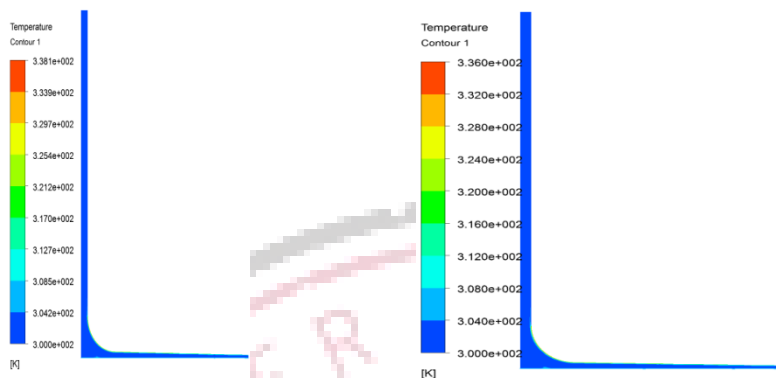


Figure 41: Temperature distribution on SCPP for with collector height $H_2 = 4$ m & $R = 20$ m at 600 W/m^2

Figure 42: Temperature distribution on SCPP for with collector height $H_2 = 4$ m & $R = 20$ m at 400 W/m^2

Solar chimney power station simulation software evaluation for baseline model with collector height $H_2 = 4$ m and solar radionuclides of 600 W/m^2 and 400 W/m^2 . As illustrated in 41 and 42, the solar thermal collector reached maximum temperatures of 338.1 K and 336.0 K . Solar chimney power station numerical modelling simulation for baseline model with collectors height $H_2 = 4$ m and solar radiations of 200 W/m^2 . Figure 43 shows that the maximum temperatures observed inside the solar chimney, which was 333.9 K .

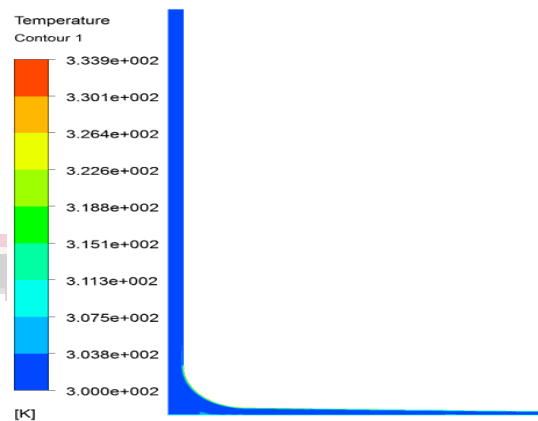


Figure 43: Temperature distribution on SCPP for with collector height $H_2 = 4$ m & $R = 20$ m at 200 W/m^2

Results for CFD analysis of solar chimney power plant at collector height 5 m and radial curvature of collector roof is 20 m:

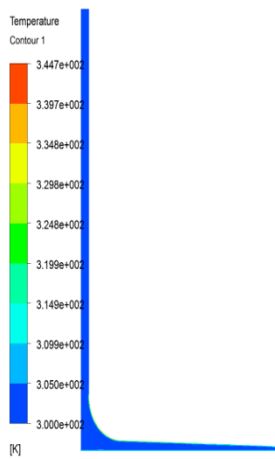


Figure 44: Temperature distribution on SCPP for with collector height $H_2 = 5$ m & $R = 20$ m at 1000 W/m^2

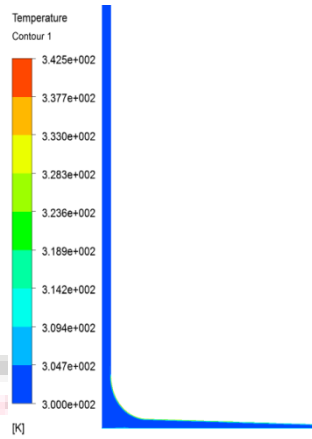


Figure 45: Temperature distribution on SCPP for with collector height $H_2 = 5$ m & $R = 20$ m at 800 W/m^2

Solar chimney power station numerical modelling simulation for base model at collector height $H_2 = 5$ m and solar radionuclides of 1000 W/m^2 and 800 W/m^2 . Figures 44 and 45 showed that maximum temperature within the solar chimney was 344.7 K for 1000 W/m^2 and 342.5 K for 800 W/m^2 .

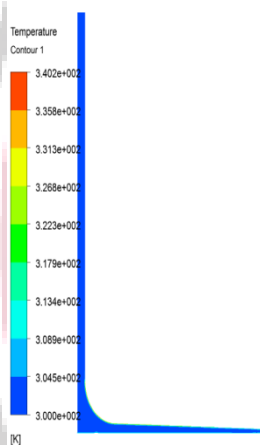


Figure 46: Temperature distribution on SCPP for with collector height $H_2 = 5$ m & $R = 20$ m at 600 W/m^2

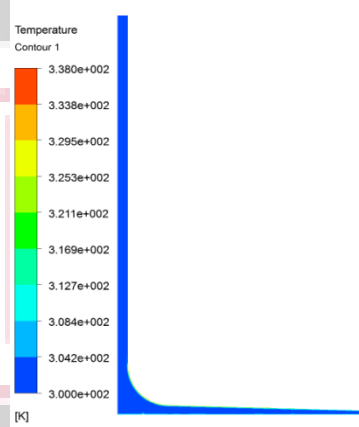


Figure 47: Temperature distribution on SCPP for with collector height $H_2 = 5$ m & $R = 20$ m at 400 W/m^2

Solar chimney power plant simulation software simulation for base model with collector height $H_2 = 5$ m and solar radioactive isotopes of 600 W/m^2 and 400 W/m^2 . As illustrated in 46 and 47, the solar thermal collector reached maximum temperatures of 340.2 K and 338.0 K .

Solar thermal power plant simulation software simulation for baseline model at collector height $H_2 = 5$ m and solar radiations of 200 W/m^2 . Figure 48 represents the highest temperatures observed inside the photovoltaic panel, which was 335.8 K .

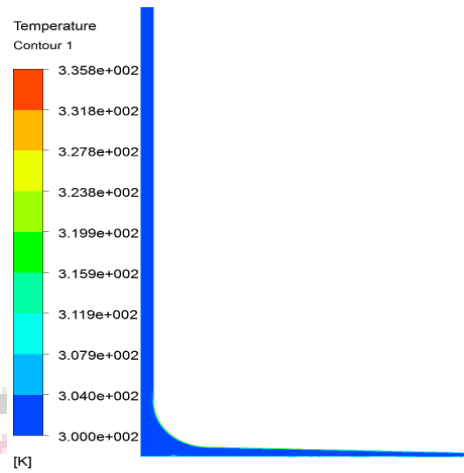


Figure 48: Temperature distribution on SCPP for with collector height $H_2 = 5$ m & $R = 20$ m at 200 W/m^2

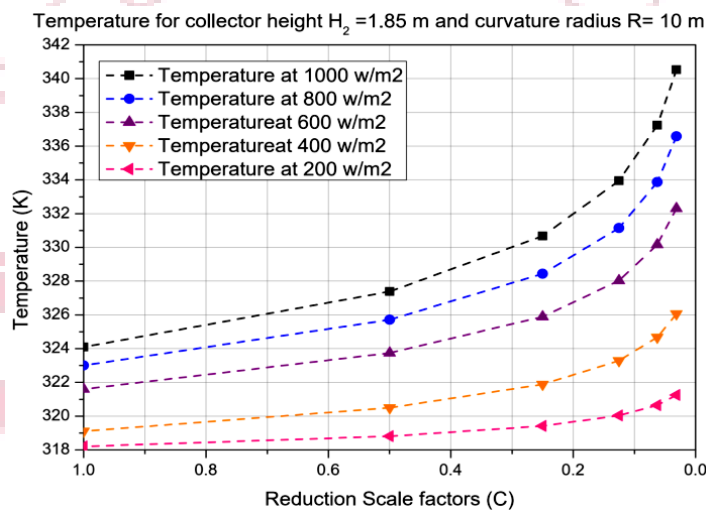


Figure 49: Temperature of SCPP at collector height $H_2 = 1.85$ m and radial curvature of collector roof is 10 m

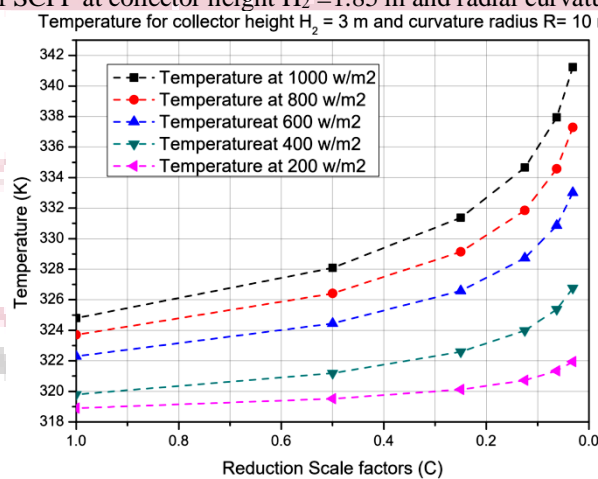


Figure 50: Temperature of SCPP at collector height $H_2 = 3$ m and radial curvature of collector roof is 10 m

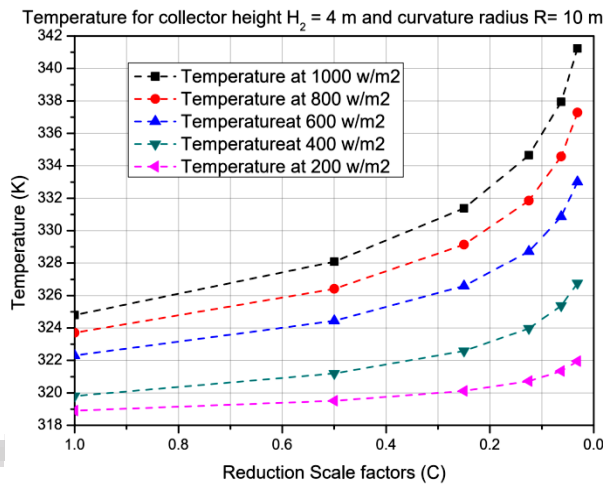


Figure 51: Temperature of SCPP at collector height $H_2 = 4$ m and radial curvature of collector roof is 10m

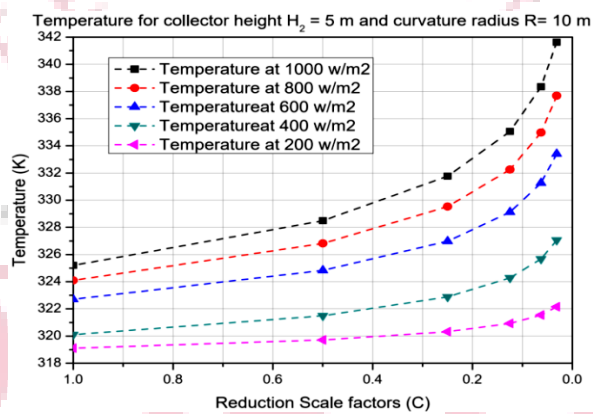


Figure 52: Temperature of SCPP at collector height $H_2 = 1.85$ m and radial curvature of collector roof is 20 m

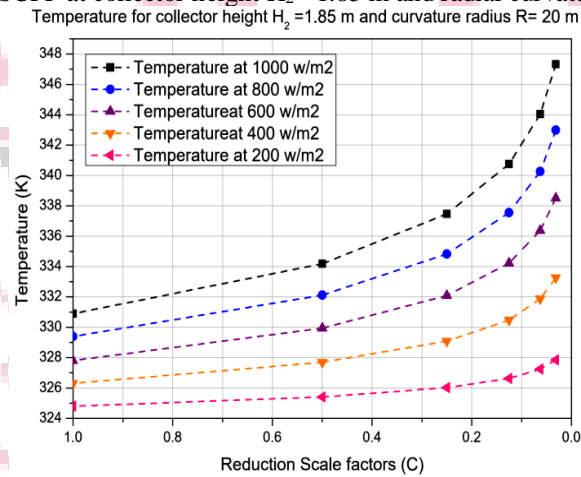


Figure 53: Temperature of SCPP at collector height $H_2 = 3$ m and radial curvature of collector roof is 20 m

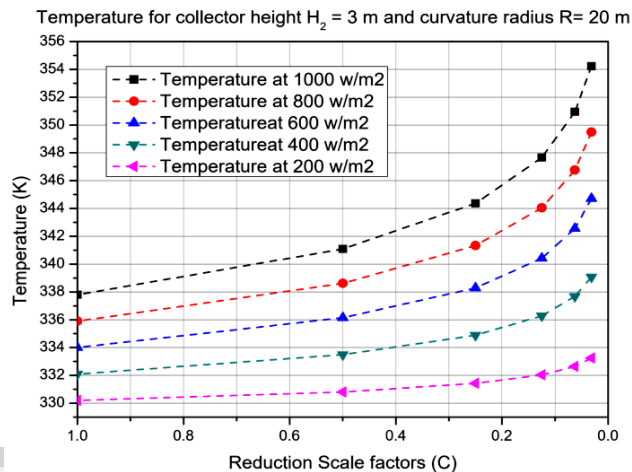


Figure 54: Temperature of SCPP at collector height $H_2 = 4$ m and radial curvature of collector roof is 20 m

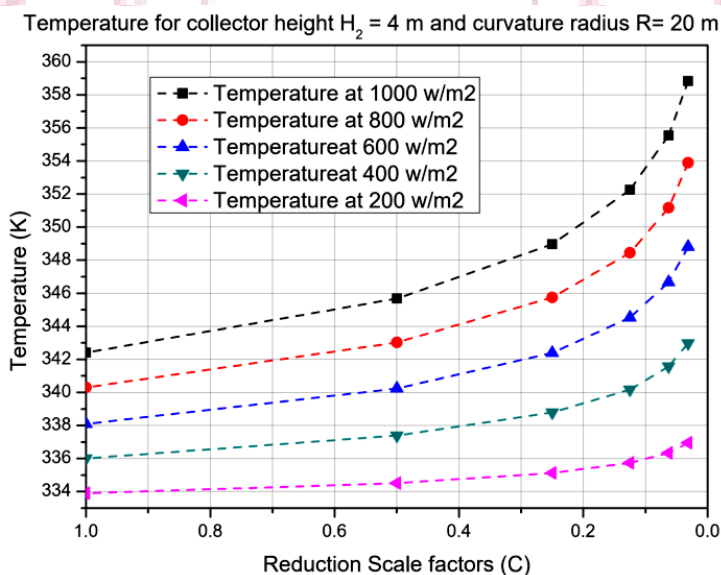


Figure 55: Temperature of SCPP at collector height $H_2 = 4$ m and radial curvature of collector roof is 20 m

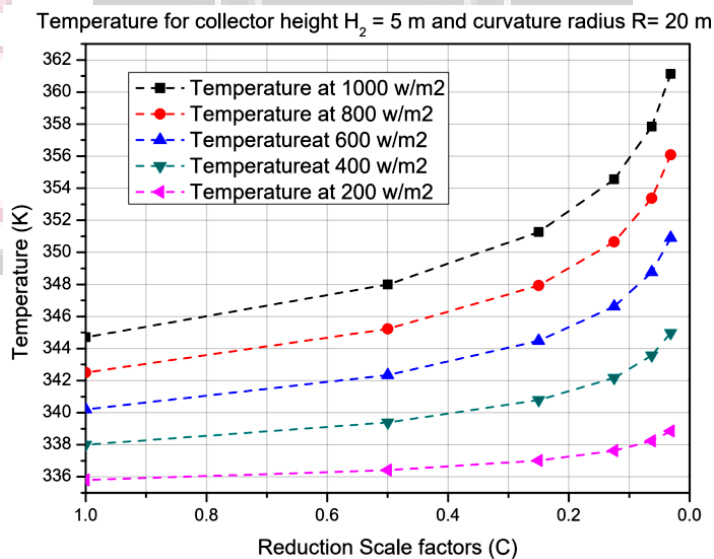


Figure 56: Temperature of SCPP at collector height $H_2 = 5$ m and radial curvature of collector roof is 20 m

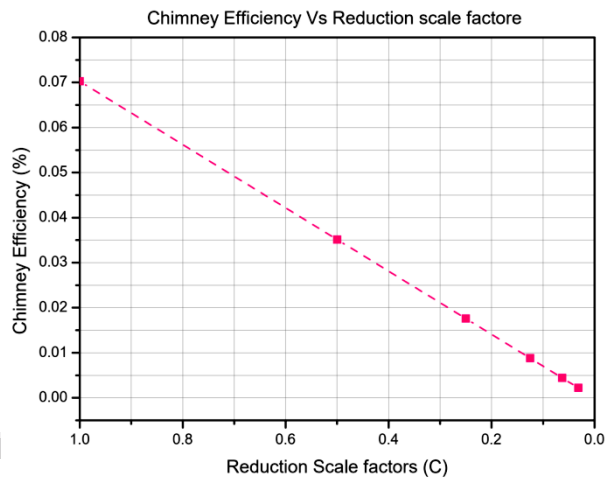


Figure 57:chimney efficiency of SCPP at different reduction scale factor

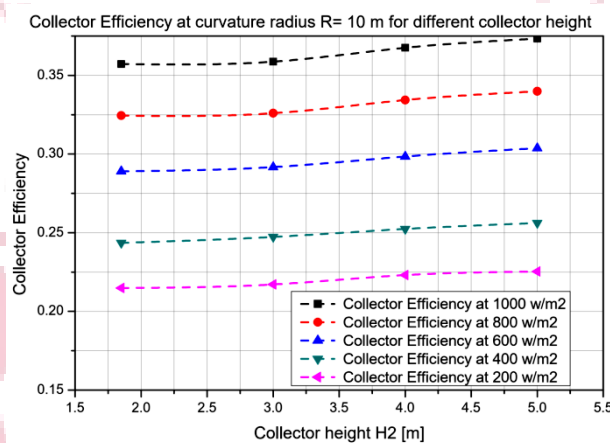


Figure 58:Collector Efficiency at curvature radius R= 10 m for different collector height

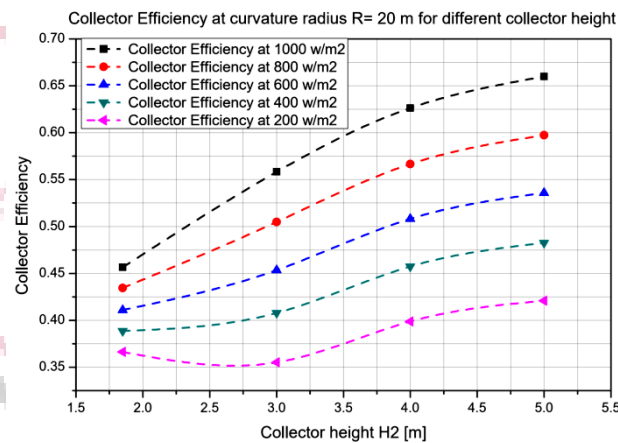


Figure 59:Collector Efficiency at curvature radius R= 20 m for different collector height

V. Conclusion

In this study, computer simulation analyses of combined heat and power plants with various outlet collection altitudes ($H_2 = 1.85\text{ m}$, 3 m , 4 m , and 5 m) and circumferential curving over collectors roofs of 10 m and 20 m were carried out. The output collection elevation is changed to change the roof angle and curving diameter of the collection, while the inlet receiver elevation is set at $H_1 = 1.85\text{ m}$ of solar water heating system at varied radiation from the sun such as 1000 W/m^2 , 800 W/m^2 , 600 W/m^2 , 400 W/m^2 , and 200 W/m^2 . From such a work, some conclusions can be inferred.

1. At varying solar irradiation, a simulation software assessment was conducted on a solar water heating system with varied collector heights H_2 of 1.85 m , 3 m , 4 m , and 5 m and a radially curving of collectors roof of 10 m . Temperature differences within the solar water heating system were measured for $C = 1$ at $H_2 = 1.85\text{ m}$ the temperature range from

324.10 K to 318.20 K, at $H_2 = 3$ m the temperature range from 324.20 K to 318.40 K, at $H_2 = 4$ m the temperature range from 324.80 K to 318.90 K & at $H_2 = 5$ m the temperature range from 325.20 K to 319.10 K. The concentration effectiveness has been noticed to range from 21.48 percent at 200 W/m² to 37.34 percent at 1000 W/m².

2. At varying solar irradiation, a simulation software assessment was conducted on a solar water heating system with varied collector heights H_2 of 1.85m, 3m, 4m, and 5m and a radial curving of collectors roof of 20 m. Temperature differences on the inside of the solar water heating system were determined for $C = 1$ for $H_2 = 1.85$ m, ranging from 330.90 K to 324.80 K, for $H_2 = 3$ m, ranging from 337.80 K to 330.20 K, for $H_2 = 4$ m, ranging from 342.40 K to 333.90 K, and for $H_2 = 5$ m, ranging from 344.70 K to 335.80 K. The collector efficiency has been shown to range from 36.64 percent at 200 W/m² to 66.00 percent at 1000 W/m².

The inclinations and curving diameter of the collectors roof effect the coefficient of performance, and the specific capacitance is highest when the collector height is $H_2 = 5$ m and the radius curving of something like the collectors roof is 20m, as shown in the following statement.

References

- [1] Ammar Mebaeki et al (2022) "CFD analysis of solar chimney power plant: Finding a relationship between model minimization and its performance for use in urban areas" *Energy Reports* 8 (2022) 500–513. <https://doi.org/10.1016/j.egy.2021.12.008>.
- [2] Omer K. Ahmed et al. (2022) "Hybrid solar chimneys: A comprehensive review" *Energy Reports* 8 (2022) 438–460. <https://doi.org/10.1016/j.egy.2021.12.007>.
- [3] Tianhe Long et al. (2022) "Experimental study on liquid desiccant regeneration performance of solar still and natural convective regenerators with/without mixed convection effect generated by solar chimney" *Energy* 239 (2022) 121919 <https://doi.org/10.1016/j.energy.2021.121919>.
- [4] Ammar Bouchair (2022) "The effect of the altitude on the performance of a solar chimney" *Energy* Volume 249, 15 June 2022, 123704 <https://doi.org/10.1016/j.energy.2022.123704>.
- [5] Seyyed Hossein Fallah & Mohammad Sadegh Valipour (2022) "Numerical investigation of a small scale sloped solar chimney power plant" *Renewable Energy* Volume 183, January 2022, Pages 1-11 <https://doi.org/10.1016/j.renene.2021.10.081>.
- [6] Cristiana Brasil Maia & Janaina de Oliveira Castro Silva (2022) "Thermodynamic assessment of a small-scale solar chimney" *Renewable Energy* Volume 186, March 2022, Pages 35-50 <https://doi.org/10.1016/j.renene.2021.12.128>.
- [7] A.T. Layeni et al. (2021) "Computational and sensitivity analysis of a dual purpose solar chimney for buildings" *Materials Today: Proceedings* 12 July 2021 <https://doi.org/10.1016/j.matpr.2021.07.292>.
- [8] Vazquez-Ruiz et al. (2021) "Effect of the solar roof chimney position on heat transfer in a room" *International Journal of Mechanical Sciences* 209 (2021) 106700 <https://doi.org/10.1016/j.ijmecsci.2021.106700>.
- [9] Carlos Mendez & Yusuf Bicer (2021) "Integration of solar chimney with desalination for sustainable water production: A thermodynamic assessment" *Case Studies in Thermal Engineering* 21 (2020) 100687. <https://doi.org/10.1016/j.csite.2020.100687>.
- [10] D.M. Aliaga et al. ((2021) "Modified solar chimney configuration with a heat exchanger: Experiment and CFD simulation" *New Journal and we have not received input yet* 22 (2021) 100850 <https://doi.org/10.1016/j.tsep.2021.100850>.
- [11] Guoqing He et al. (2021) "Ventilation performance of solar chimney in a test house: Field measurement and validation of plume model" *Building and Environment* 193 (2021) 107648 <https://doi.org/10.1016/j.buildenv.2021.107648>.
- [12] Haihua Zhang et al. (2021) "A wall solar chimney to ventilate multi-zone buildings" *Sustainable Energy Technologies and Assessments* 47 (2021) 101381 <https://doi.org/10.1016/j.seta.2021.101381>.
- [13] Lu Zuo et al. (2021) "Effect of chimney shadow on the performance of wind supercharged solar chimney power plants: A numerical case study for the Spanish prototype" *Volume 4 Number 4 August 2021 (405-414)* DOI: 10.14171/j.2096-5117.gei.2021.04.006.
- [14] Mohammad Reza Torabi et al. (2021) "Investigation the performance of solar chimney power plant for improving the efficiency and increasing the outlet power of turbines using computational fluid dynamics" *Energy Reports* 7 (2021) 4555–4565 <https://doi.org/10.1016/j.egy.2021.07.044>.
- [15] Mukundjee Pandey et al. (2021) "Performance analysis of a waste heat recovery solar chimney for nocturnal use" *Engineering Science and Technology, an International Journal* 24 (2021) 1–10 <https://doi.org/10.1016/j.jestch.2020.11.009>
- [16] Parisa Rahdan et al. (2021) "Simulation and geometric optimization of a hybrid system of solar chimney and water desalination" *Energy Conversion and Management* 243 (2021) 114291 <https://doi.org/10.1016/j.enconman.2021.114291>.
- [17] Rizgar Bakr Weli et al. (2021) "Investigation of the performance parameters of a sloped collector solar chimney model e An adaptation for the North of Iraq" *Renewable Energy* 176 (2021) 504e519 <https://doi.org/10.1016/j.renene.2021.05.075>.
- [18] Saman Rashidi et al. (2021) "Assessment of solar chimney combined with phase change materials" *Journal of the Taiwan Institute of Chemical Engineers* 000 (2021) 110 <https://doi.org/10.1016/j.jtice.2021.03.001>.

- [19] Suhaib J. Shbailat et al. (2021) "Possible energy saving of evaporative passive cooling using a solar chimney of metal foam porous absorber" *Energy Conversion and Management*: X 12 (2021) 100118 <https://doi.org/10.1016/j.ecmx.2021.100118>.
- [20] Yan Cao et al. (2021) "Single solar chimney technology as a natural free ventilator; energy-environmental case study for Hong Kong" *Case Studies in Thermal Engineering* 26 (2021) 101173 <https://doi.org/10.1016/j.csite.2021.101173>.
- [21] Yang Liu et al. (2021) "Mitigating air pollution strategies based on solar chimneys" *Solar Energy* 218 (2021) 11–27 <https://doi.org/10.1016/j.solener.2021.02.021>
- [22] AjeetPratap Singh et al. (2020) "Performance enhancement strategies of a hybrid solar chimney power plant integrated with photovoltaic panel" *Energy Conversion and Management* 218 (2020) 113020 <https://doi.org/10.1016/j.enconman.2020.113020>.
- [23] C. Jimenez-Xaman et al. (2020) "Assessing the thermal performance of a rooftop solar chimney attached to a single room" *Journal of Building Engineering* 31 (2020) 101380 <https://doi.org/10.1016/j.jobe.2020.101380>.

